

Considering Bending and Vibration of Homogeneous Nanobeam Coated by a FG Layer

H. Salehipour^{1,*}, M. Jamshidi¹, A. Shahsavari²

¹Department of Mechanical Engineering, Ilam University, Ilam 69315-516, Iran

²Department of Mechanical Engineering, Kermanshah University of Technology, Kermanshah, Iran

Received 12 March 2020; accepted 11 May 2020

ABSTRACT

In this research static deflection and free vibration of homogeneous Nano beams coated by a functionally graded (FG) layer is investigated according to the nonlocal elasticity theory. A higher order beam theory is used that does not need the shear correction factor. The equations of motion (equilibrium equations) are extracted by using Hamilton's principle. The material properties are considered to vary in the thickness direction of FG coated layer. This nonlocal Nano beam model incorporates the length scale parameter (nonlocal parameter) that can capture the small-scale effects. In the numerical results section, the effects of different parameters, especially the ratio of thickness of FG layer to the total thickness of the beam are considered and discussed. The results reveal that the frequency is maximum for a special value of material power index. In addition, increasing the ratio of thickness of FG layer to the total thickness of the beam increases the static deflection and decreases the natural frequencies. These results help with the understanding such coated structures and designing them carefully. The results also show that the new nonlocal FG Nano beam model produces larger vibration and smaller deflection than homogeneous nonlocal Nano beam.

© 2020 IAU, Arak Branch. All rights reserved.

Keywords : Nano beam; Nonlocal elasticity; FG coating; Free vibration; Static deflection.

1 INTRODUCTION

SINCE the discovery of carbon nanotubes by Iijima [1] in 1991, nanostructures have been increasingly used due to their large Young's modulus, yield strength, flexibility, and conductivity properties (Zhang, Wang, Duan, Xiang, & Zong, [2]). Nanostructures can be modeled using the molecular dynamics or the continuum mechanics. Compared to the molecular dynamics model, the continuum mechanics approach is widely used due to its computational efficiency and simplicity. Due to the presence of small scale effects at the nano scale, size dependent continuum mechanics models such as the strain gradient theory (Nix & Gao, [3]), couple stress theory (Hadjesfandiari & Dargush, [4]), modified couple stress theory (Asghari, Kahrobaian, & Ahmadian, [5]; Ma, Gao,

*Corresponding author.

E-mail address: h.salehipour@ilam.ac.ir (H. Salehipour).

& Reddy, [6]; Reddy, [7]), and nonlocal elasticity theory (Eringen, [8]; Eringen & Edelen, [9]; Eringen, [10]) are used. Among these theories, the nonlocal elasticity theory initiated by Eringen is widely used. Unlike the local theories which assume that the stress at a point is a function of strain at that special point, the nonlocal elasticity theory assumes that the stress at a given point is a function of strains at all points in the continuum. (Huu-Tai Thai, [11]). Nonlocal elasticity has been used to study wave propagation in composites, elastic waves, dislocation mechanics, the dynamic and static analysis of carbon nanotubes and nanorods (A.C. Eringen,[12]; A.C. Eringen,[13]; A.C. Eringen, [14]; A.C. Eringen, [15]; J. Peddieson, [16]; L.J. Sudak, [17]; M.C. Ece, [18]; P. Lu, H.P. Lee, C. Lu, P.Q. Zhang, [19]; M. Aydogdu, [20]). Molecular dynamic simulations and nonlocal continuum models were compared for wave propagation in single- and double-walled carbon nanotubes (Y. Hu, K.M. Liew, Q. Wang, X.Q. He, B.I. Yakobson,[21]) and the elastic buckling of single layered graphene sheet(A. Sakhae-Pour,[22]). Good agreement was observed between the molecular dynamic simulations and the nonlocal continuum modeling. (Metin Aydogdu, [23]). In the classical (local) elasticity theory, the stress at a given point depends only on the strain at the same point whereas in the nonlocal elasticity theory, the stress at a point is a function of strains at all points in the continuum. In this way, the nonlocal continuum theory contains information about the long range forces between atoms, and the internal length scale is introduced into the constitutive equations including a material parameter to capture the small scale effect. In this context, the application of the classical continuum theory to the analysis of nanostructures is not appropriate since the classical theory lacks the accountability for the size effects arising from the small-scale. (M. Simsek, H.H. Yurtcu, [24]). A functionally graded material (FGM) is described by a continuous material variant in one or more dimensions by steadily changing the microstructure from one material to another for the optimum distribution of component materials. FGMs present numerous profits (Byrd & Birman, [25]) including the improved stress spreading, the enhanced thermal resistance, the higher fracture toughness, and the inferior stress intensity factors that introduce them as very eye-catching choices in various engineering fields. This category of materials affords the specific profits of both ingredients (O.Rahmani, O.Pedram, [26]). Functionally graded materials are such desirable ones that would be used in industrial applications variously such as, biomedicines, electronics, optics, etc.; therefore, this huge amount of requirements have made researchers to study this topic more. (Ebrahimi, F., A. Rastgoo, and A. Atai, [27]; Ebrahimi, F., M.H. Naei, and A. Rastgoo,[28]; Ghadiri, M., et al,[29]; Navvab Shafiei, Majid Ghadiri & Mohammad Mahinzare ,[30]). Following the development of the material technology, functionally graded materials, FGM, are extensively used. Reddy (Reddy JN, Chin CD, [31]) and Praveen (Praveen GN, Reddy JN, [32]) studied the thermo-mechanical behavior of FG plates. They used a through-the-thickness variation of the material properties according to a power law. FGMs are used in micro/ nano-electro-mechanical system (MEMS/NEMS) and atomic force microscopes (AFMs) to achieve a high-level sensitivity and the desired performance. Pisano et al. (Pisano AA, Sofi A, Fuschi P, [33]; Pisano AA, Sofi A, Fuschi P ,[34]) exploited the nonlocal finite element method for analyzing homogeneous and nonhomogeneous nonlocal elastic 2D problems.(M.A.Eltaher,Samir A, Emam,F.F.Mahmoud,[35]). Song et al. (Song M., Yang J., Kitipornchai S,[36]) investigated the static bending and compressive buckling behavior of FG multilayered plates reinforced by graphene nanoplatelets by using the FSDT and the Halpin-Tsai micromechanical model. The effect of graphene platelets on the thermal buckling and post buckling analyses of FG multilayered nanocomposite plates was investigated by Wu et al. (Wu H., Kitipornchai S., Yang J.,[37]) according to the FSDT. FGMs offer great promise in applications where the operating conditions are severe. For example, wear-resistant linings for handling large heavy abrasive ore particles, rocket heat shields, heat exchanger tubes, thermoelectric generators, heat-engine components, plasma facings for fusion reactors, and electrically insulating metal/ceramic joints. The mechanical and thermal response of materials with spatial gradients in composition and microstructure is of considerable interest in numerous technological areas such as tribology, optoelectronics, biomechanics, nanotechnology and high temperature technology. They are also ideal for minimizing thermo-mechanical mismatch in metal-ceramic bonding. Gradations in microstructure are also commonly found in biological cellular materials such as wood and bone, where biological adaptation has distributed the strongest microstructure in regions that experience the highest stress. Functionally graded materials are produced using the advanced manufacturing techniques, including powder metallurgy, chemical vapor deposition, centrifugal casting, and so on. Today the development of mechanical and electronic systems in a compact case such as micro-electro-mechanical-systems (MEMS) has become more important, because this essential part of technology increases the speed and compact size of industrial equipment (Ali Khanchehgardan, Ghader Rezazadeh, Rasoul Shabani,[38]). In the earlier research, the material properties of the nanobeam were taken as homogeneous and isotropic. Very recently, the Nano beam made of functionally graded materials (FGMs) received extensive attention, which represents a type of composite materials made of two or more different materials. Now the FGMs have broadly spread into MEMS and NEMS, which endows MEMS and NEMS with more sensitive and advanced functionalities. Their effective properties can be tailored with smooth changing. In contrast, the combing properties of laminated composites vary suddenly. The mechanical properties of FGM

structures, such as buckling, post-buckling, free vibration, forced vibration and thermal vibration have been extensively studied (Zhen W, Wanji C,[39];;Reddy J,[40];Ke L-L, Wang Y-S, Yang J, Kitipornchai S.,[41];Jia X, Ke L, Feng C, Yang J, Kitipornchai S.[42];Li L, Hu Y.,[43]; Chen D, Yang J, Kitipornchai S. ,[44]; Arbind A, Reddy J. ,[45]; Reddy J. ,[46]; Yang J, Wu H, Kitipornchai S. ,[47]; Wu H, Kitipornchai S, Yang J. ,[48]; Simsek M,[49]; Simsek M, Yurtcu H ,[24]; Ke L-L, Yang J, Kitipornchai S, Wang Y-S ,[50]; Ke L-L, Yang J, Kitipornchai S, Bradford MA. ,[51]; Kitipornchai S, Ke L, Yang J, Xiang Y.,[52]; Farokhi H, Ghayesh MH, Gholipour A. ,[53]; Shafiei N, Kazemi M. ,[54]; Lee JW, Lee JY. , [55]). It is noted that, in most published researches, the material properties of the FGMs were assumed to vary in one direction. Obviously, this is not ideal; the unidirectional FG structures may not be suitable for various complex engineering applications. Some multi-directional FG materials may be required, which can provide great flexibility in the design of advanced devices (Tianzhi Yang, Ye Tang, Qian Li, Xiao-Dong Yang,[56]). Variation in material properties through the thickness of FGM plates or beams results in quite different behaviors for plates or beams made of pure materials under both static and dynamic loading conditions. For example, bifurcation buckling generally cannot occur for FGM plates or beams with simply supported edges due to in plane loading. Transverse deflection is initiated, regardless of the magnitude of the loading, as is often the case with laminated composite materials (Leissa AW, [57]; Leissa AW, [58]; Qatu MS, Leissa AW,[59]). Shen (Shen HS, [60] and Aydogdu (Aydogdu M, [61] considered the phenomenon. Shen (Shen HS, [60]) stated that bifurcation buckling does not take place for FGM rectangular plates with simply supported edges due to the bending–stretching coupling. In the past, several analyses had been reported concerning the buckling of FGM plates, which cannot exist physically, as pointed out by Qatu and Leissa (Qatu MS, Leissa AW, [59]). The flatness conditions of an FGM plate during the pre-buckling stage were presented by Aydogdu (Aydogdu M, [61]). However, few researchers have further studied these special behaviors of FGM plates or beams in detail. Shen (Shen HS, [62]) analyzed the influence of various factors such as thermal loading and in plane boundary conditions on the nonlinear bending of FGM plates. Nonlinear bending and post-buckling of an FGM circular plate under a thermal loading and uniform radial pressure, respectively, were investigated by Ma and Wang (Ma LS, Wang TJ, [63]; Ma LS, Wang TJ, [64]). They found that transverse deflections occur immediately when an in-plane compressive load is applied to a simply supported FGM circular plate (S. Ma, D.W. Lee, [65]).

In general, in this paper the free vibration and static bending of homogeneous Nano beams coated by a functionally graded (FG) layer is presented by using the nonlocal elasticity theory. The homogeneous structures coated by FG layers are used widely in industrial applications, but a few studies considered their mechanical behaviors. Unlike the local theory, the nonlocal elasticity considered that stress at a given point is not only dependent on the strain at that point, but is a function of strain at the neighboring points. The equations of motion are procured by nonlocal differential constitutive relations of Eringen and Hamilton’s principle. The material properties of FG layer are defined by power-law form. In the numerical results section, the effects of different parameters, especially the ratio of thickness of FG layer to the total thickness of beam are considered and discussed.

2 MATHEMATICAL FORMULATION

2.1 Nonlocal beam theories

Eringen first introduced nonlocal beam theory. The nonlocal theory states that the stress at a point x' not only depends on the strain at the same point but also on strains on those all points of the body. Nonlocal stress tensor σ at point x is expressed by:

$$\sigma = \int_V (k |x - x'|, \tau) s(x') dx \tag{1}$$

where k is $s(x')$ the classical macroscopic stress tensor at point is x' , he nonlocal modulus or kernel function, $|x - x'|$ is the Euclidean distance, and τ is a material constant as define $\tau = \frac{e_0 a}{L}$ where a is an internal characteristic length parameter and e_0 is a constant appropriate to each material and L is the external characteristic length. The simple form of nonlocal constitute relations is proposed by Eringen as:

$$\sigma_x - \mu \frac{d^2 \sigma_x}{dx^2} = E(z) \epsilon_x \tag{2a}$$

$$\sigma_{xz} - \mu \frac{d^2 \sigma_{xz}}{dx^2} = G(z) \gamma_{xz} \tag{2b}$$

where $\mu = (e_0 a)^2$ is the nonlocal parameter, E and $G = \frac{E}{2(1+\nu)}$ are the elastic and shear modulus of the beam (where ν is the Poisson's ratio), σ_{xx} and ϵ_{xx} are the axial stress and strain, σ_{xz} and γ_{xz} are the shear stress and strain. When the nonlocal parameter is taken zero ($e_0 a = 0$), the constitutive relations of the local classical continuum theory is obtained. Choice of $e_0 a$ is crucial to ensure the validity of nonlocal FG Nano beam. A conservative estimate of the scale coefficient $e_0 a < 2.00nm$ for a single wall carbon nanotube is proposed (Wang & Wang [66]).

2.2 Functionally graded material

Fig. 1 shows a functionally graded simply supported beam of length L , width b and thickness h . The material properties of beam vary continuously through the thickness direction. The thickness of the homogenous part is h_0 and the thickness of the FG material is $h - h_0$. In general, the distribution of a material property P through the thickness can be given as:

$$P(z) = \begin{cases} P_s & -h/2 \leq z \leq h_0 - h/2 \\ (P_a - P_s) \left(\frac{z - (h_0 - h/2)}{h - h_0} \right)^k + P_s & h_0 - h/2 \leq z \leq h/2 \end{cases} \tag{3}$$

where k is the non-negative number that it is the power law exponent which dictates the material variation profile through the thickness of the beam. P_a and P_s are the material properties of alumina and steel. $P(z)$ can be expressed in terms of the young's modulus, density and shear modulus as follows:

$$E(z) = \begin{cases} E_s & -h/2 \leq z \leq h_0 - h/2 \\ (E_a - E_s) \left(\frac{z - (h_0 - h/2)}{h - h_0} \right)^k + E_s & h_0 - h/2 \leq z \leq h/2 \end{cases} \tag{3a}$$

$$\rho(z) = \begin{cases} \rho_s & -h/2 \leq z \leq h_0 - h/2 \\ (\rho_a - \rho_s) \left(\frac{z - (h_0 - h/2)}{h - h_0} \right)^k + \rho_s & h_0 - h/2 \leq z \leq h/2 \end{cases} \tag{3b}$$

$$G(z) = \begin{cases} G_s & -h/2 \leq z \leq h_0 - h/2 \\ (G_a - G_s) \left(\frac{z - (h_0 - h/2)}{h - h_0} \right)^k + G_s & h_0 - h/2 \leq z \leq h/2 \end{cases} \tag{3b}$$

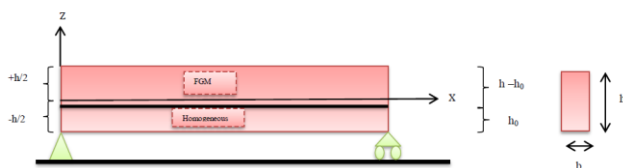


Fig.1 Schematic of the FG Nano beam.

2.3 Kinematics

In this survey, the Nano beam displacement theory is as follows:

$$u_1(x, z, t) = u(x, t) - z \left(\frac{dw_b}{dx} \right) + \left[\frac{1}{4}z - \frac{5}{3}z \left(\frac{z}{h} \right)^2 \right] \frac{dw_s}{dx} \quad (4a)$$

$$u_2(x, z, t) = 0 \quad (4b)$$

$$u_3(x, z, t) = w_b(x, t) + w_s(x, t) \quad (4c)$$

where u , w_b and w_s are the axial displacement, bending and shear components of transverse displacement, respectively. Then nonzero axial and shear strains are given as:

$$\varepsilon_x = \frac{du}{dx} - z \frac{d^2w_b}{dx^2} - f \frac{d^2w_s}{dx^2} \quad (5a)$$

$$\gamma_{xz} = g \frac{dw_s}{dx} \quad (5b)$$

where

$$f = -\frac{z}{4} + \frac{5}{3}z \left(\frac{z}{h} \right)^2 \quad (6a)$$

$$g = 1 - \frac{df}{dz} = \frac{5}{4} - 5 \left(\frac{z}{h} \right)^2 \quad (6b)$$

2.4 Equations of motion

The governing equations will be obtained by using Hamilton's principle:

$$\int_0^T (\delta U + \delta V - \delta K) dt = 0 \quad (7)$$

where δU , δV and δK are the variation of strain, potential and kinetic energy, respectively.

The Hamilton Principle states that the total kinetic, potential and strain energy in a certain period is equal to 0. With regard to minimum energy principle, if a small change is made in a system in a short period, the system will return back to its previous condition and will remain stable. The variation of strain energy is given as:

$$\delta U = \int_0^L \int_A (\sigma_x \delta \varepsilon_x + \sigma_{xz} \delta \gamma_{xz}) dA dx = \int_0^L (N \frac{d\delta u}{dx} - M_b \frac{d^2\delta w_b}{dx^2} - M_s \frac{d^2\delta w_s}{dx^2} + Q \frac{d\delta w_s}{dx}) dx \quad (8)$$

where N is the axial normal force, Q is the shear force; M_b and M_s are the bending and shear components of moment. These stress resultants are defined as:

$$N = \int_A \sigma_x dA \quad (9a)$$

$$M_b = \int_A z \sigma_x dA \quad (9b)$$

$$M_s = \int_A f \sigma_x dA \quad (9c)$$

$$Q = \int_A g \sigma_{xz} dA \quad (9d)$$

The variation of potential energy is given as:

$$\delta \mathcal{V} = - \int_0^L q \delta(w_b + w_s) dx \quad (10)$$

where q is the transverse load.

The variation of kinetic energy is given as:

$$\begin{aligned} \delta K = \int_0^L \int_A \rho(z) (\dot{u}_1 \delta \dot{u}_1 + \dot{u}_3 \delta \dot{u}_3) dA dx = \int_0^L [& I_0 (\dot{u} \delta \dot{u} + (\dot{w}_b + \dot{w}_s) \delta (\dot{w}_b + \dot{w}_s)) - I_1 (\dot{u} \frac{d \delta \dot{w}_b}{dx} + \delta \dot{u} \frac{d \dot{w}_b}{dx}) \\ & - I_2 (\dot{u} \frac{d \delta \dot{w}_s}{dx} + \delta \dot{u} \frac{d \dot{w}_s}{dx}) + I_3 \frac{d \dot{w}_b}{dx} \frac{d \delta \dot{w}_b}{dx} + I_4 \frac{d \dot{w}_s}{dx} \frac{d \delta \dot{w}_s}{dx} + I_5 (\frac{d \dot{w}_b}{dx} \frac{d \delta \dot{w}_s}{dx} + \frac{d \dot{w}_s}{dx} \frac{d \delta \dot{w}_b}{dx})] dx \end{aligned} \quad (11)$$

where dot-superscript above the displacement parameters shows the derivative with respect to the time variable t . I_0 , I_1 , I_2 , I_3 , I_4 and I_5 can be obtained as follows:

$$I_0 = \int_A \rho(z) dA \quad (12a)$$

$$I_1 = \int_A z \rho(z) dA \quad (12b)$$

$$I_2 = \int_A f \rho(z) dA \quad (12c)$$

$$I_3 = \int_A z^2 \rho(z) dA \quad (12d)$$

$$I_4 = \int_A f^2 \rho(z) dA \quad (12e)$$

$$I_5 = \int_A fz \rho(z) dA \quad (12f)$$

Substituting the Eqs. (8), (10) and (11) into Eq. (7) and integrating by parts and totalize the coefficients of δu , $\delta \dot{w}_b$ and $\delta \dot{w}_s$, the following equations are taken:

$$\frac{dN}{dx} = I_0 \ddot{u} - I_1 \frac{d \dot{w}_b}{dx} - I_2 \frac{d \dot{w}_s}{dx} \quad (13a)$$

$$\frac{d^2 M_b}{dx^2} + q = I_0 (\ddot{w}_b + \ddot{w}_s) + I_1 \frac{d \ddot{u}}{dx} - I_3 \frac{d^2 \dot{w}_b}{dx^2} - I_5 \frac{d^2 \dot{w}_s}{dx^2} \quad (13b)$$

$$\frac{d^2 M_s}{dx^2} + \frac{dQ}{dx} + q = I_0 (\ddot{w}_b + \ddot{w}_s) + I_2 \frac{d \ddot{u}}{dx} - I_4 \frac{d^2 \dot{w}_s}{dx^2} - I_5 \frac{d^2 \dot{w}_b}{dx^2} \quad (13c)$$

In addition, the boundary conditions are extracted as follows:

$$N=0 \text{ or } u=0 \quad (14a)$$

$$w_b = 0 \text{ or } V_b = \frac{dM_b}{dx} - I_1 \ddot{u} + I_3 \frac{d\ddot{w}_b}{dx} + I_5 \frac{d\ddot{w}_s}{dx} = 0 \quad (14b)$$

$$w_s = 0 \text{ or } V_s = \frac{dM_s}{dx} + Q - I_2 \ddot{u} + I_4 \frac{d\ddot{w}_s}{dx} + I_5 \frac{d\ddot{w}_b}{dx} = 0 \quad (14c)$$

$$\frac{dw_b}{dx} = 0 \text{ or } M_b = 0 \quad (14d)$$

$$\frac{dw_s}{dx} = 0 \text{ or } M_s = 0 \quad (14e)$$

Substituting Eq. (5) into Eq. (2) and then substituting the results into Eq. (9), the stress resultants are taken as:

$$N - \mu \frac{d^2 N}{dx^2} = J_0 \frac{du}{dx} - J_1 \frac{d^2 w_b}{dx^2} - J_2 \frac{d^2 w_s}{dx^2} \quad (15a)$$

$$M_b - \mu \frac{d^2 M_b}{dx^2} = J_1 \frac{du}{dx} - J_3 \frac{d^2 w_b}{dx^2} - J_4 \frac{d^2 w_s}{dx^2} \quad (15b)$$

$$M_s - \mu \frac{d^2 M_s}{dx^2} = J_2 \frac{du}{dx} - J_4 \frac{d^2 w_b}{dx^2} - J_5 \frac{d^2 w_s}{dx^2} \quad (15c)$$

$$Q - \mu \frac{d^2 Q}{dx^2} = J_6 \frac{dw_s}{dx} \quad (15d)$$

where $J_0, J_1, J_2, J_3, J_4, J_5$ and J_6 can be obtained as follows:

$$J_0 = \int_A E(z) dA \quad (16a)$$

$$J_1 = \int_A z E(z) dA \quad (16b)$$

$$J_2 = \int_A f E(z) dA \quad (16c)$$

$$J_3 = \int_A z^2 E(z) dA \quad (16d)$$

$$J_4 = \int_A f z E(z) dA \quad (16e)$$

$$J_5 = \int_A f^2 E(z) dA \quad (16f)$$

$$J_6 = \int_A g^2 G(z) dA \quad (16g)$$

The nonlocal equations of motion can be obtained in terms of displacement by substituting Eq. (15) into Eq. (13) as:

$$J_0 \frac{d^2 u}{dx^2} - J_1 \frac{d^3 w_b}{dx^3} - J_2 \frac{d^3 w_s}{dx^3} = I_0 (\ddot{u} - \mu \frac{d^2 \ddot{u}}{dx^2}) - I_1 (\frac{d \ddot{w}_b}{dx} - \mu \frac{d^3 \ddot{w}_b}{dx^3}) - I_2 (\frac{d \ddot{w}_s}{dx} - \mu \frac{d^3 \ddot{w}_s}{dx^3}) \quad (17a)$$

$$J_1 \frac{d^3 u}{dx^3} - J_3 \frac{d^4 w_b}{dx^4} - J_4 \frac{d^4 w_s}{dx^4} + q - \mu \frac{d^2 q}{dx^2} = I_0 ((\ddot{w}_b + \ddot{w}_s) - \mu \frac{d^2 (\ddot{w}_b + \ddot{w}_s)}{dx^2}) \\ + I_1 (\frac{d \ddot{u}}{dx} - \mu \frac{d^3 \ddot{u}}{dx^3}) - I_3 (\frac{d^2 \ddot{w}_b}{dx^2} - \mu \frac{d^4 \ddot{w}_b}{dx^4}) - I_5 (\frac{d^2 \ddot{w}_s}{dx^2} - \mu \frac{d^4 \ddot{w}_s}{dx^4}) \quad (17b)$$

$$J_2 \frac{d^3 u}{dx^3} - J_4 \frac{d^4 w_b}{dx^4} - J_5 \frac{d^4 w_s}{dx^4} + J_6 \frac{d^2 w_s}{dx^2} + q - \mu \frac{d^2 q}{dx^2} = I_0 ((\ddot{w}_b + \ddot{w}_s) - \mu \frac{d^2 (\ddot{w}_b + \ddot{w}_s)}{dx^2}) \\ + I_2 (\frac{d \ddot{u}}{dx} - \mu \frac{d^3 \ddot{u}}{dx^3}) - I_4 (\frac{d^2 \ddot{w}_s}{dx^2} - \mu \frac{d^4 \ddot{w}_s}{dx^4}) - I_5 (\frac{d^2 \ddot{w}_b}{dx^2} - \mu \frac{d^4 \ddot{w}_b}{dx^4}) \quad (17c)$$

3 ANALYTICAL SOLUTION FOR STATIC BENDING AND VIBRATION OF A SIMPLY_SUPPORTED FG NANOBEAM

For simply supported Nano beam with length L , the boundary conditions are:

$$w_b = w_s = M_b = M_s = 0 \quad \text{at } x = 0, L \quad (18)$$

The displacement fields are assumed as follows:

$$u(x, t) = \sum_{n=1}^{\infty} u_m e^{i \alpha x} \cos \alpha x \quad (19a)$$

$$w_b(x, t) = \sum_{n=1}^{\infty} w_{bn} e^{i \alpha x} \sin \alpha x \quad (19b)$$

$$w_s(x, t) = \sum_{n=1}^{\infty} w_{sn} e^{i \alpha x} \sin \alpha x \quad (19c)$$

where $i = \sqrt{-1}$ is the imaginary number, $\alpha = \frac{n\pi}{L}$, u_m , w_{bn} and w_{sn} are coefficients and ω is the natural frequency. The transverse load q is given by the Fourier sinusoidal series as:

$$q(x) = \sum_{n=1}^{\infty} Q_n \sin \alpha x \quad (20)$$

where Q_n are the Fourier coefficients and are given for uniform load $q(x) = q_0$ as follows:

$$Q_n = \frac{2}{L} \int_0^L q(x) \sin \alpha x dx = \frac{4q_0}{n\pi} \quad (n = 1, 3, 5, \dots) \quad (21)$$

By substituting the displacement fields and transverse load q from Eq. (19), (20) into Eq. (17) into equations of motion, the following equations can be obtained as:

$$\left(\begin{bmatrix} -J_0 \alpha^2 & -J_1 \alpha^3 & -J_2 \alpha^3 \\ J_1 \alpha^3 & J_3 \alpha^4 & J_4 \alpha^4 \\ J_2 \alpha^3 & J_4 \alpha^4 & J_5 \alpha^4 + J_6 \alpha^2 \end{bmatrix} - \lambda \omega^2 \begin{bmatrix} -I_0 & -I_1 \alpha & -I_2 \alpha \\ I_1 \alpha & I_0 + I_3 \alpha^2 & I_0 + I_5 \alpha^2 \\ I_2 \alpha & I_0 + I_5 \alpha^2 & I_0 + I_4 \alpha^2 \end{bmatrix} \right) \begin{Bmatrix} u_m \\ w_{bn} \\ w_{sn} \end{Bmatrix} = \begin{Bmatrix} 0 \\ \lambda Q_n \\ \lambda Q_n \end{Bmatrix} \quad (22)$$

From above equation, the transverse displacement under static loading ($\omega = 0$), and natural frequencies of free vibration ($Q_n = 0$) are extracted.

4 NUMEERICAL RESULTS

In this section, the numerical results for the previous sections are presented. The shear correction factor is taken 5/6 and modulus of elasticity, Poisson’s ratio and density of materials of the beam in the Table 1. are shown. The length of the Nano beam is assumed 10 nm. Non-dimensional fundamental frequency and non-dimensional deflection relations are given as follows:

$$\hat{\omega}_1 = \omega L^2 \sqrt{\frac{\rho_s A}{E_s I}} \tag{23}$$

$$\hat{w} = \frac{100(w_2 + w_3)E_s I}{q_0 L^4} \tag{24}$$

Table 1
Material properties of FGM constituent.

Properties	Steel	Alumina(Al_2O_3)
E	210(GPa)	390(GPa)
ρ	7800(Kg/m ³)	3960(Kg/m ³)
ν	0.3	0.24

Tables 2-7 present the fundamental frequency for different ratio h_0/h and power exponent k , and the results compared for $h/L = 0.2, 0.1, 0.05$ and 0.01 , and nonlocal parameter $\mu = 0, 1, 2, 3$ and $4(nm^2)$. By increasing the nonlocal parameter, fundamental frequency decreases and by increasing h/L fundamental frequency increases. In addition, by increasing the h_0/h , the fundamental frequency decreases. For a constant value of k , by increasing nonlocal parameter, the value of static bending will increase and the frequency will reduce. Accordingly, changes in the nonlocal parameter affect the physical quality. Fundamental frequency decreases versus increasing the nonlocal parameter (Figs. 2 to 5).

In addition, the minimum of fundamental frequency is for homogeneous Nano beam (Table 8, Fig. 6). Table 9 presents the fundamental frequency for $h/L = 0.1$ and $\mu = 2$. In addition, Fig. 7 shows the variation of fundamental frequency versus the power low index of FG properties. In addition, the results compared different value of h_0/h and k . This observation is produced for $h/L = 0.05$ and $\mu = 2$ (Table 10). It is seen that the frequency is the maximum when the power index k is equal to one.

In the Table 11 and Table 12, the fundamental frequency is examined for $h/L = 0.1, k = 1$ and $h/L = 0.05, k = 1$ and different values of h_0/h and μ . As shown in Fig. 9, by increasing the nonlocal parameter the fundamental frequency is decreasing while the h/L and k remain unchanged, and the fundamental frequency decreases when the h_0/h increases. Table 13 listed the fundamental frequency for $k = 1$ and $\mu = 1$ and different values of h_0/h . Fig. 8 shows the variation of fundamental frequency versus h_0/h for $k = 1$ and $\mu = 1$. The frequency decreases by increasing the h_0/h .

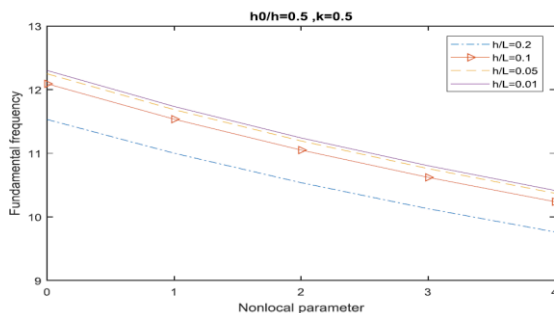


Fig.2
Variation of fundamental frequency versus nonlocal parameter for $h_0/h = 0.5$ and $k = 0.5$.

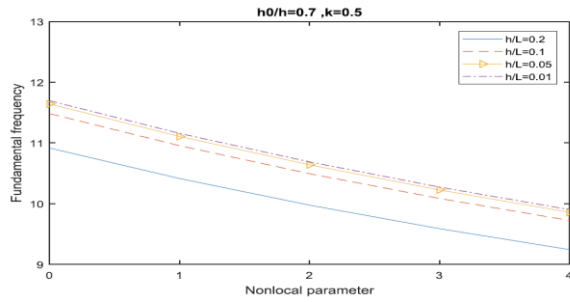


Fig.3
Variation of fundamental frequency versus nonlocal parameter for $h_0/h=0.7$ and $k=0.5$.

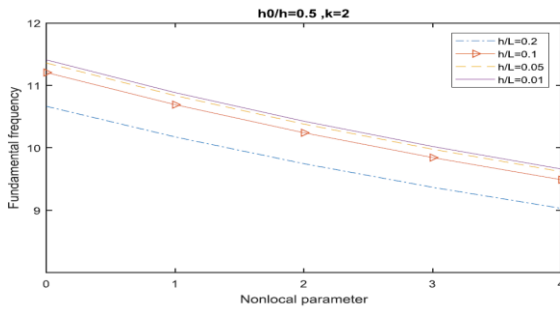


Fig.4
Variation of fundamental frequency versus nonlocal parameter for $h_0/h=0.5$ and $k=2$.

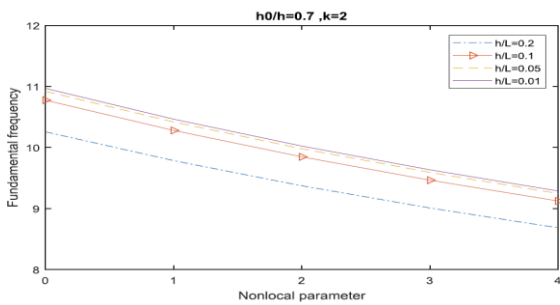


Fig.5
Variation of fundamental frequency versus nonlocal parameter for $h_0/h=0.7$ and $k=2$.

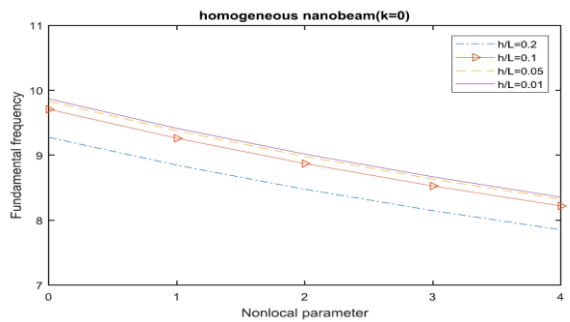


Fig.6
Variation of fundamental frequency versus nonlocal parameter for homogeneous nanobeam.

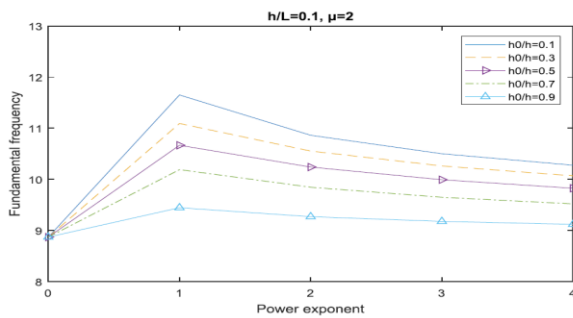


Fig.7
Variation of fundamental frequency versus power exponent for $h/L=0.1$ and $\mu=2$.

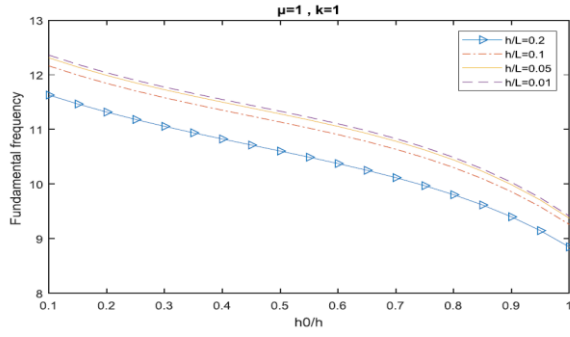


Fig.8
Variation of fundamental frequency versus h_0/h for $\mu=1$ and $k=1$.

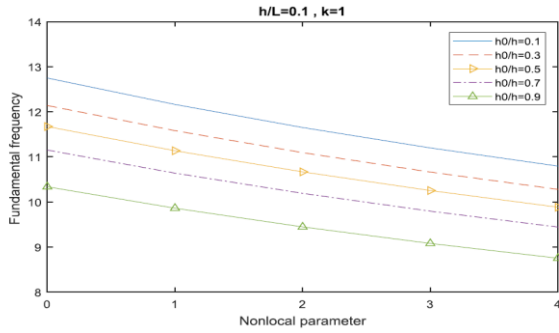


Fig.9
Variation of fundamental frequency versus nonlocal parameter for $h/L=0.1$ and $k=1$.

Table 2
Nondimensional fundamental frequency versus nonlocal parameter for $h_0/h=0.5$ and $k=0.5$.

h/L	$\mu (nm^2)$	Fundamental frequency
0.2	0	11.5303
	1	11.0003
	2	10.5372
	3	10.1280
	4	9.7631
0.1	0	12.0914
	1	11.5355
	2	11.0499
	3	10.6208
	4	10.2382
0.05	0	12.2484
	1	11.6853
	2	11.1933
	3	10.7587
	4	10.3711
0.01	0	12.3002
	1	11.7348
	2	11.2407
	3	10.8043
	4	10.4150

Table 3
Nondimensional fundamental frequency versus nonlocal parameter for $h_0/h=0.7$ and $k=0.5$.

h/L	$\mu (nm^2)$	Fundamental frequency
0.2	0	10.9156
	1	10.4138
	2	9.9754
	3	9.5880
	4	9.2426

0.1	0	11.4824
	1	10.9545
	2	10.4933
	3	10.0859
	4	9.7225
0.05	0	11.6419
	1	11.1067
	2	10.6391
	3	10.2260
	4	9.8576
0.01	0	11.6947
	1	11.1571
	2	10.6874
	3	10.2724
	4	9.9023

Table 4Nondimensional fundamental frequency versus nonlocal parameter for $h_0/h=0.5$ and $k=1$.

h/L	μ (nm^2)	Fundamental frequency
0.2	0	11.1153
	1	10.6043
	2	10.1579
	3	9.7635
	4	9.4117
0.1	0	11.6721
	1	11.1355
	2	10.6667
	3	10.2525
	4	9.8831
0.05	0	11.8283
	1	11.2845
	2	10.8094
	3	10.3897
	4	10.0154
0.01	0	11.8799
	1	11.3338
	2	10.8566
	3	10.4351
	4	10.0591

Table 5Nondimensional fundamental frequency versus nonlocal parameter for $h_0/h=0.7$ and $k=1$.

h/L	μ (nm^2)	Fundamental frequency
0.2	0	10.6050
	1	10.1174
	2	9.6915
	3	9.3152
	4	8.9796
0.1	0	11.1510
	1	10.6384
	2	10.1905
	3	9.7948
	4	9.4419
0.05	0	11.3046
	1	10.7849
	2	10.3308
	3	9.9297
	4	9.5719

0.01	0	11.3554
	1	10.8333
	2	10.3773
	3	9.9743
	4	9.6150

Table 6

Nondimensional fundamental frequency versus nonlocal parameter for $h_0/h=0.5$ and $k=2$.

h/L	$\mu (nm^2)$	Fundamental frequency
0.2	0	10.6640
	1	10.1738
	2	9.7455
	3	9.3671
	4	9.0296
0.1	0	11.2060
	1	10.6909
	2	10.2408
	3	9.8432
	4	9.4885
0.05	0	11.3583
	1	10.8361
	2	10.3799
	3	9.9769
	4	9.6174
0.01	0	11.4086
	1	10.8842
	2	10.4260
	3	10.0211
	4	9.6601

Table 7

Nondimensional fundamental frequency versus nonlocal parameter for $h_0/h=0.7$ and $k=2$.

h/L	$\mu (nm^2)$	Fundamental frequency
0.2	0	10.2560
	1	9.7845
	2	9.3726
	3	9.0086
	4	8.6841
0.1	0	10.7743
	1	10.2790
	2	9.8463
	3	9.4640
	4	9.1230
0.05	0	10.9198
	1	10.4178
	2	9.9792
	3	9.5918
	4	9.2462
0.01	0	10.9679
	1	10.4637
	2	10.0232
	3	9.6340
	4	9.2869

Table 8Nondimensional fundamental frequency versus nonlocal parameter for $k=0$ (homogeneous beam).

h/L	$\mu (nm^2)$	Fundamental frequency
0.2	0	9.27452
	1	8.84816
	2	8.47566
	3	8.14656
	4	7.85305
0.1	0	9.70751
	1	9.26124
	2	8.87135
	3	8.52689
	4	8.21967
0.05	0	9.82813
	1	9.37631
	2	8.98158
	3	8.63284
	4	8.32180
0.01	0	9.86793
	1	9.41429
	2	9.01795
	3	8.66780
	4	8.35550

Table 9Nondimensional fundamental frequency versus power exponent for $h/L=0.1$ and $\mu=2$.

h_0/h	k	Fundamental frequency
0.1	0	8.8714
	1	11.6508
	2	10.8627
	3	10.5013
	4	10.2771
0.2	0	8.8714
	1	11.3448
	2	10.7038
	3	10.3835
	4	10.1761
0.3	0	8.8714
	1	11.0932
	2	10.5533
	3	10.2628
	4	10.0693
0.5	0	8.8714
	1	10.6667
	2	10.2408
	3	9.9933
	4	9.8261
0.7	0	8.8714
	1	10.1905
	2	9.8463
	3	9.6498
	4	9.5209
0.9	0	8.8714
	1	9.4457
	2	9.2705
	3	9.1780
	4	9.1205

Table 10
Nondimensional fundamental frequency versus power exponent for $h_0/L=0.05$ and $\mu=2$.

h_0/h	k	Fundamental frequency
0.1	0	8.9816
	1	11.7930
	2	11.0023
	3	10.6402
	4	10.4147
0.2	0	8.9816
	1	11.4850
	2	10.8434
	3	10.5221
	4	10.3130
0.3	0	8.9816
	1	11.2333
	2	10.6932
	3	10.4009
	4	10.2052
0.5	0	8.9816
	1	10.8094
	2	10.3799
	3	10.1286
	4	9.9581
0.7	0	8.9816
	1	10.3308
	2	9.9792
	3	9.7782
	4	9.6462
0.9	0	8.9816
	1	9.5692
	2	9.3897
	3	9.2950
	4	9.2362

Table 11
Nondimensional fundamental frequency versus nonlocal parameter for $h_0/L=0.1$ and $k=1$.

h_0/h	$\mu (nm^2)$	Fundamental frequency
0.1	0	12.7490
	1	12.1629
	2	11.6508
	3	11.1985
	4	10.7950
0.2	0	12.4141
	1	11.8434
	2	11.3448
	3	10.9043
	4	10.5114
0.3	0	12.1387
	1	11.5807
	2	11.0932
	3	10.6624
	4	10.2783
0.5	0	11.6721
	1	11.1355
	2	10.6667
	3	10.2525
	4	9.8831

0.7	0	11.1510
	1	10.6384
	2	10.1905
	3	9.7948
	4	9.4419
0.9	0	10.3360
	1	9.8608
	2	9.4457
	3	9.0790
	4	8.7518

Table 12Nondimensional fundamental frequency versus nonlocal parameter for $h/L=0.05$ and $k=1$.

h_0/h	μ (nm^2)	Fundamental frequency
0.1	0	12.9046
	1	12.3113
	2	11.7930
	3	11.3351
	4	10.9267
0.2	0	12.5675
	1	11.9898
	2	11.4850
	3	11.0391
	4	10.6413
0.3	0	12.2921
	1	11.7270
	2	11.2333
	3	10.7972
	4	10.4081
0.5	0	11.8283
	1	11.2845
	2	10.8094
	3	10.3897
	4	10.0154
0.7	0	11.3046
	1	10.7849
	2	10.3308
	3	9.9297
	4	9.5719
0.9	0	10.4711
	1	9.9898
	2	9.5692
	3	9.1976
	4	8.8663

Table 13Nondimensional fundamental frequency versus h_0/h for $\mu=1$ and $k=1$.

h/L	h_0/h	Fundamental frequency
0.2	0.3	11.0565
	0.5	10.6043
	0.7	10.1174
	0.9	9.4003
	1	8.8482
0.1	0.3	11.5807
	0.5	11.1355
	0.7	10.6384
	0.9	9.8608
	1	9.2612
0.05	0.3	11.7270
	0.5	11.2845
	0.7	10.7849

	0.9	9.9898
	1	9.3763
0.01	0.3	11.7753
	0.5	11.3338
	0.7	10.8333
	0.9	10.0324
	1	9.4143

Tables 14-21 show the nondimensional deflection for different ratio h_0/h and value of k , and the results are compared for different ratio h/L and nonlocal parameter μ . The values of nondimensional deflection are calculated by using 100 terms in series in Eqs. (19) and (20) that has a good convergence. By increasing the nonlocal parameter the nondimensional deflection increases and through increasing the ratio h/L , the nondimensional deflection decreases. By increasing the ratio h_0/h , the deflection increases and with increasing the value of k , the deflection increases (Figs. 10-13). It can be seen that the maximum value of deflection is for the homogeneous nanobeam (Fig. 14). In Fig. 15, the variation of non-dimensional deflection versus the power index is shown for $h/L=0.1$ and $\mu=2$, and the results are compared for different values of h_0/h and k , this examination is procured for $h/L=0.05$ and $\mu=2$ (Table 22).

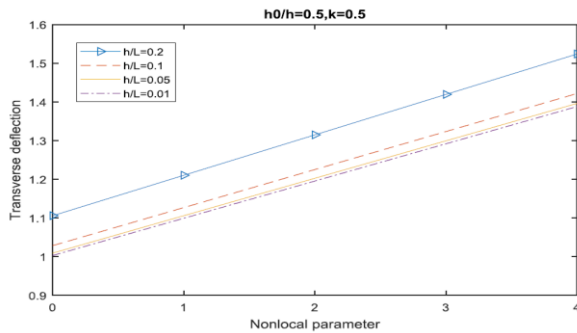


Fig.10
Variation of non-dimensional deflection versus nonlocal parameter for $h_0/h=0.5$ and $k=0.5$.

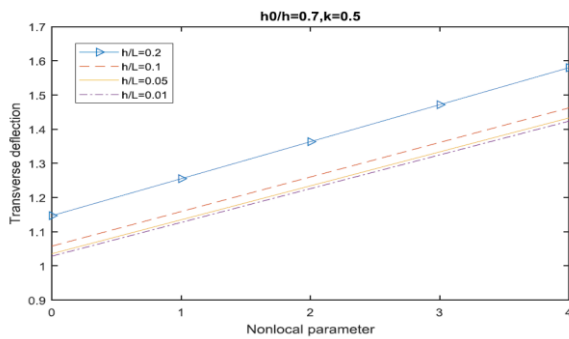


Fig.11
Variation of non-dimensional deflection versus nonlocal parameter for $h_0/h=0.7$ and $k=0.5$.

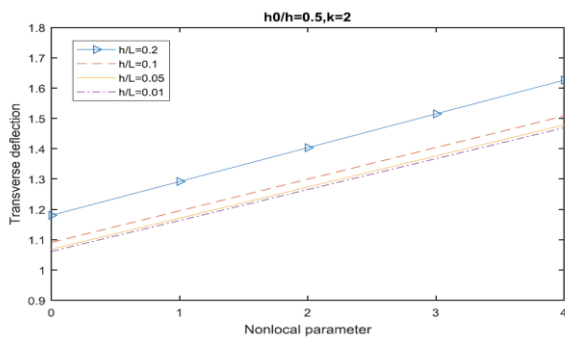


Fig.12
Variation of non-dimensional deflection versus nonlocal parameter for $h_0/h=0.5$ and $k=2$.

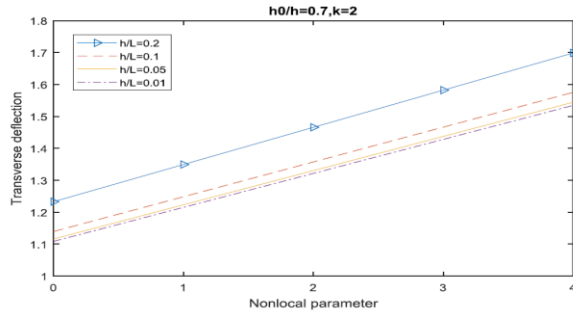


Fig.13
Variation of non-dimensional deflection versus nonlocal parameter for $h_0/h=0.7$ and $k=2$.

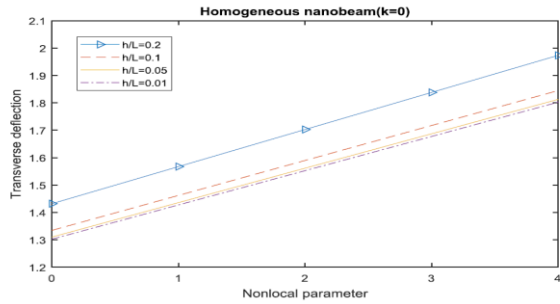


Fig.14
Variation of non-dimensional deflection versus nonlocal parameter for homogeneous Nano beam.

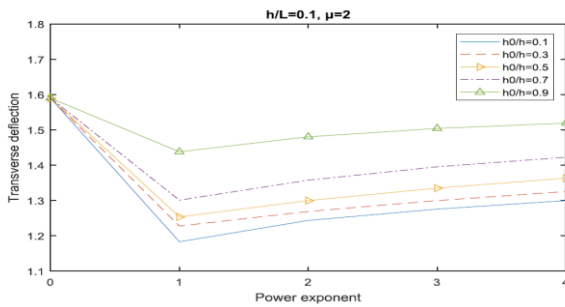


Fig.15
Variation of non-dimensional deflection versus power exponent for $h/L=0.1$ and $\mu=2$.

Table 14
Non-dimensional deflection versus nonlocal parameter for $h_0/h=0.5$ and $k=0.5$.

h/L	μ (nm^2)	Non-dimensional deflection
0.2	0	1.1057
	1	1.2102
	2	1.3147
	3	1.4192
	4	1.5237
0.1	0	1.0284
	1	1.1267
	2	1.2250
	3	1.3233
	4	1.4216
0.05	0	1.0090
	1	1.1058
	2	1.2025
	3	1.2993
	4	1.3960
0.01	0	1.0028
	1	1.0991
	2	1.1953
	3	1.2916
	4	1.3879

Table 15

Non-dimensional deflection versus nonlocal parameter for $h_0/h=0.7$ and $k=0.5$.

h/L	$\mu (nm^2)$	Non-dimensional deflection
0.2	0	1.1470
	1	1.2552
	2	1.3634
	3	1.4716
	4	1.5799
0.1	0	1.0580
	1	1.1591
	2	1.2602
	3	1.3612
	4	1.4623
0.05	0	1.0357
	1	1.1350
	2	1.2343
	3	1.3336
	4	1.4329
0.01	0	1.0286
	1	1.1273
	2	1.2261
	3	1.3248
	4	1.4235

Table 16

Non-dimensional deflection versus nonlocal parameter for $h_0/h=0.5$ and $k=1$.

h/L	$\mu (nm^2)$	Non-dimensional deflection
0.2	0	1.1360
	1	1.2433
	2	1.3505
	3	1.4578
	4	1.5651
0.1	0	1.0524
	1	1.1529
	2	1.2535
	3	1.3541
	4	1.4547
0.05	0	1.0314
	1	1.1303
	2	1.2292
	3	1.3281
	4	1.4270
0.01	0	1.0247
	1	1.1231
	2	1.2215
	3	1.3198
	4	1.4182

Table 17

Non-dimensional deflection versus nonlocal parameter for $h_0/h=0.7$ and $k=1$.

h/L	$\mu (nm^2)$	Non-dimensional deflection
0.2	0	1.1836
	1	1.2953
	2	1.4069
	3	1.5186
	4	1.6303
0.1	0	1.0922
	1	1.1965
	2	1.3009
	3	1.4053
	4	1.5096

0.05	0	1.0693
	1	1.1718
	2	1.2744
	3	1.3769
	4	1.4794
0.01	0	1.0620
	1	1.1639
	2	1.2659
	3	1.3678
	4	1.4698

Table 18Non-dimensional deflection versus nonlocal parameter for $h_0/h=0.5$ and $k=2$.

h/L	$\mu (nm^2)$	Non-dimensional deflection
0.2	0	1.1806
	1	1.2920
	2	1.4034
	3	1.5149
	4	1.6263
0.1	0	1.0911
	1	1.1953
	2	1.2996
	3	1.4038
	4	1.5081
0.05	0	1.0687
	1	1.1711
	2	1.2736
	3	1.3761
	4	1.4785
0.01	0	1.0615
	1	1.1634
	2	1.2653
	3	1.3672
	4	1.4691

Table 19Non-dimensional deflection versus nonlocal parameter for $h_0/h=0.7$ and $k=2$.

h/L	$\mu (nm^2)$	Non-dimensional deflection
0.2	0	1.2331
	1	1.3495
	2	1.4659
	3	1.5823
	4	1.6987
0.1	0	1.1397
	1	1.2486
	2	1.3575
	3	1.4665
	4	1.5754
0.05	0	1.1163
	1	1.2234
	2	1.3304
	3	1.4375
	4	1.5445
0.01	0	1.1089
	1	1.2153
	2	1.3217
	3	1.4282
	4	1.5346

Table 20

Non-dimensional deflection versus nonlocal parameter for $k=0$ (homogeneous beam).

h/L	$\mu (nm^2)$	Non-dimensional deflection
0.2	0	1.43195
	1	1.56735
	2	1.70275
	3	1.83815
	4	1.97355
0.1	0	1.33458
	1	1.46217
	2	1.58977
	3	1.71737
	4	1.84497
0.05	0	1.31021
	1	1.43586
	2	1.56151
	3	1.68716
	4	1.81281
0.01	0	1.30241
	1	1.42743
	2	1.55246
	3	1.67749
	4	1.80251

Table 21

Non-dimensional deflection versus power exponent for $h/L=0.1$ and $\mu=2$.

h_0/h	k	Non-dimensional deflection
0.1	0	1.5898
	1	1.1831
	2	1.2435
	3	1.2756
	4	1.2997
0.2	0	1.5898
	1	1.2096
	2	1.2566
	3	1.2870
	4	1.3115
0.3	0	1.5898
	1	1.2275
	2	1.2689
	3	1.2998
	4	1.3254
0.5	0	1.5898
	1	1.2535
	2	1.2996
	3	1.3351
	4	1.3631
0.7	0	1.5898
	1	1.3009
	2	1.3575
	3	1.3954
	4	1.4225
0.9	0	1.5898
	1	1.4380
	2	1.4803
	3	1.5040
	4	1.5192

Table 22
Non-dimensional deflection versus power exponent for $h/L=0.05$ and $\mu=2$.

h_0/h	k	Non-dimensional deflection
0.1	0	1.5615
	1	1.1633
	2	1.2208
	3	1.2511
	4	1.2742
0.2	0	1.5615
	1	1.1889
	2	1.2331
	3	1.2619
	4	1.2856
0.3	0	1.5615
	1	1.2058
	2	1.2445
	3	1.2741
	4	1.2990
0.5	0	1.5615
	1	1.2292
	2	1.2736
	3	1.3084
	4	1.3361
0.7	0	1.5615
	1	1.2744
	2	1.3304
	3	1.3680
	4	1.3950
0.9	0	1.5615
	1	1.4104
	2	1.4526
	3	1.4762
	4	1.4913

For a constant value of the nonlocal parameter, by increasing value of k the value of static bending will reduce and the value of fundamental frequency will increase. The power-law exponent has a great influence on the responses of FG Nano beam, and the responses can be controlled by choosing the proper values of the power-law exponent (Simsek M, Yurtcu H, [24]). Table 23 presents the variation of non-dimensional deflection for $h/L=0.1$ and $k=1$ and the results are compared for different values of h_0/h and μ . These observations are taken in Table 24 for $h/L=0.05$ and $k=1$. Fig. 16 clears the variation of non-dimensional deflection versus the nonlocal parameter. Fig. 17 shows the variation of non-dimensional deflection versus the ratio h_0/h . It is seen that by increasing the ratio h_0/h , the deflection increases and the rigidity of the beam decreases. Timoshenko's theory considers the coincidence effect of shear deformation and bending moment. In the beam theory used in this article (Huu-Tai Thai, [11]), the effects have been examined separately, so the results have a higher accuracy when compared to the Timoshenko's theory. This theory does not need the correction factor. There are some discrepancies between the frequencies, by decreasing the thickness of the beam the resulting discrepancies reduce and this is due to the shear effect which cannot be captured by Euler–Bernoulli model (O.Rahmani, O.Pedram, [26]).

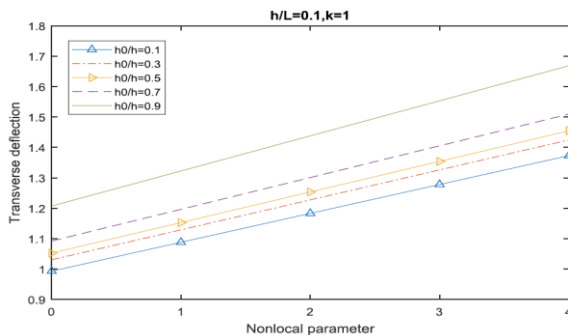


Fig.16
Variation of non-dimensional deflection versus nonlocal parameter for $h/L=0.1$ and $k=1$.

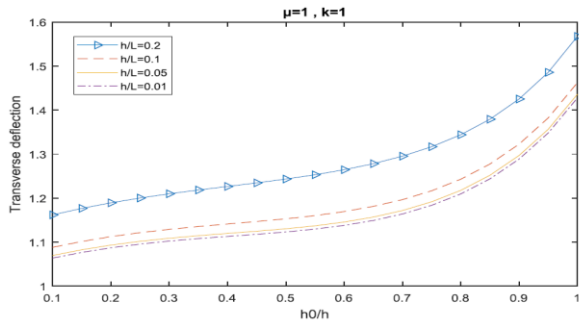


Fig.17
Variation of non-dimensional deflection versus h_0/h for $\mu=1$ and $k=1$.

Table 23
Non-dimensional deflection versus nonlocal parameter for $h/L=0.1$ and $k=1$.

h_0/h	$\mu (nm^2)$	Non-dimensional deflection
0.1	0	0.9931
	1	1.0881
	2	1.1831
	3	1.2781
	4	1.3730
0.2	0	1.0154
	1	1.1125
	2	1.2096
	3	1.3067
	4	1.4037
0.3	0	1.0305
	1	1.1290
	2	1.2275
	3	1.3261
	4	1.4246
0.5	0	1.0524
	1	1.1529
	2	1.2535
	3	1.3541
	4	1.4547
0.7	0	1.0922
	1	1.1965
	2	1.3009
	3	1.4053
	4	1.5096
0.9	0	1.2072
	1	1.3226
	2	1.4380
	3	1.5533
	4	1.6687

Table 24
Non-dimensional deflection versus nonlocal parameter for $h/L=0.05$ and $k=1$.

h_0/h	$\mu (nm^2)$	Non-dimensional deflection
0.1	0	0.9760
	1	1.0696
	2	1.1633
	3	1.2569
	4	1.3505
0.2	0	0.9976
	1	1.0932
	2	1.1889
	3	1.2846
	4	1.3802

0.3	0	1.0118
	1	1.1088
	2	1.2058
	3	1.3029
	4	1.3999
0.5	0	1.0314
	1	1.1303
	2	1.2292
	3	1.3281
	4	1.4270
0.7	0	1.0693
	1	1.1718
	2	1.2744
	3	1.3769
	4	1.4794
0.9	0	1.1834
	1	1.2969
	2	1.4104
	3	1.5239
	4	1.6374

Tables 25-28 indicate the comparison of fundamental frequency and non-dimensional deflection in different values of h/L with references O.Rahmani, O.Pedram [26] and Simsek M., Yurtcu H., [24]. A good agreement between the results illustrates the validation of the presented formulation and the numerical results. For the lower thickness to length ratio, the results are more accurate.

Table 25Non-dimensional fundamental frequency versus nonlocal parameter $k=0.5$.

h/L	μ (nm^2)	Ref.O.Rahmani [26]	Present
0.05	0	7.7149	7.7151
	1	7.3602	7.3604
	2	7.0504	7.0506
	3	6.7766	6.7768
	4	6.5325	6.5327
0.02	0	7.7413	7.7414
	1	7.3854	7.3855
	2	7.0745	7.0745
	3	6.7998	6.7999
	4	6.5548	6.5549
0.01	0	7.7451	7.7451
	1	7.3891	7.3891
	2	7.0780	7.0780
	3	6.8032	6.8032
	4	6.5580	6.5581

Table 26Non-dimensional fundamental frequency versus nonlocal parameter $k=1$.

h/L	μ (nm^2)	Ref.O.Rahmani [26]	Present
0.05	0	6.9676	6.9676
	1	6.6473	6.6473
	2	6.3674	6.3675
	3	6.1202	6.1202
	4	5.8997	5.8997
0.02	0	6.9917	6.9917
	1	6.6703	6.6703
	2	6.3895	6.3895
	3	6.1414	6.1414
	4	5.9201	5.9201

	0	6.9952	6.9952
	1	6.6736	6.6736
0.01	2	6.3927	6.3927
	3	6.1444	6.1445
	4	5.9231	5.9231

Table 27
Non-dimensional deflection versus power exponent for $e_0a=0$ (nm).

h/L	k	Ref. Simsek. M [24]	Present
	0	5.3383	5.3383
0.1	1	2.4194	2.4194
	3	1.9249	1.9234
	10	1.5799	1.5790
	0	5.2227	5.2228
	1	2.3732	2.3732
0.03	3	1.8894	1.8892
	10	1.5489	1.5488
	0	5.2096	5.2096
	1	2.3679	2.3679
0.01	3	1.8853	1.8854
	10	1.5453	1.5454

Table 28
Non-dimensional deflection versus power exponent for $e_0a=1$ (nm).

h/L	k	Ref. Simsek. M [24]	Present
	0	5.8487	5.8487
0.1	1	2.6508	2.6508
	3	2.1091	2.1074
	10	1.7310	1.7301
	0	5.2784	5.2785
0.03	1	2.3985	2.3985
	3	1.9095	1.9094
	10	1.5654	1.5653
	0	5.2146	5.2146
0.01	1	2.3702	2.3702
	3	1.8871	1.8872
	10	1.5468	1.5469

5 CONCLUSION

In the present study vibration and static bending of nonlocal homogeneous Nano beam coated by FG layers was analyzed by the nonlocal higher order shear deformation beam theory. The equations of motion were derived using the Hamilton's principle. The material properties were considered to vary in the thickness direction of FG coated layer. This nonlocal Nano beam model incorporates the length scale parameter (nonlocal parameter) that can capture the small scale effects. In the numerical results section, the effects of different parameters, especially the ratio of the thickness of FG layer to the total thickness of the beam was investigated. The results revealed that the increasing the ratio of thickness of FG layer to the total thickness of beam increases the static deflection and decreases the natural frequencies, respectively. These results help with the understanding of such coated structures and designing them carefully. The results also show that the new nonlocal FG Nano beam model produces larger vibration and smaller deflection than the homogeneous nonlocal Nano beam. The results of this article can be used as a benchmark for the static deflection and free vibration of homogeneous plate coated by FG layers.

REFERENCES

- [1] Iijima S., 1991, Helical Microtubules of Graphitic Carbon, *Nature* 354: 56-58.
- [2] Zhang Y.Y., Wang C. M., Duan W.H., Xiang Y., Zong Z., 2009, Assessment of continuum mechanics models in predicting buckling strains of single walled carbon nanotubes, *Nanotechnology* 20: 395707.

- [3] Nix W.D., GAO H., 1998, Indentation size effects in crystalline materials: A law for strain gradient plasticity, *Journal of the Mechanics and Physics of Solids* **46**: 411-425.
- [4] Hadesfandiari A.R., Dargush G.F., 2011, Couple stress theory for solids, *International Journal of Solids and Structures* **48**: 2496-2510.
- [5] Asghari M., Kahrobaian M.H., Ahmadian M.T., 2010, A nonlinear Timoshenko beam formulation based on the modified couple stress theory, *International Journal of Engineering Science* **48**: 1749-1761.
- [6] Ma H.M., GAO X.L., Reddy J.N., 2008, A microstructure-dependent Timoshenko beam model based on a modified couple stress theory, *Journal of Mechanics Physics and Solids* **56**: 3379-3391.
- [7] Reddy J., 2011, Microstructure-dependent couple stress theories of functionally graded beams, *Journal of the Mechanics and Physics of Solids* **59**(11): 2382-2399.
- [8] Eringen A.C., 1972, Nonlocal polar elastic continua, *International Journal of Engineering Science* **10**: 1-16.
- [9] Eringen A.C., Edelen D.G.B., 1972, On nonlocal elasticity, *International Journal of Engineering Science* **10**: 233-248.
- [10] Eringen A.C., 1983, On differential equations of nonlocal elasticity and solutions of screw dislocation and surface waves, *Journal of Applied Physics* **54**: 4703.
- [11] Thai H-T., 2012, A nonlocal beam theory for bending, buckling, and vibration of nanobeams, *International Journal of Engineering Science* **52**: 56-64.
- [12] Eringen A.C., 1972, Nonlocal polar elastic continua, *International Journal of Engineering Science* **10**: 1-16.
- [13] Eringen A.C., Edelen D.G.B., 1972, On non-local elasticity, *International Journal of Engineering Science* **10**: 230.
- [14] Eringen A.C., 1983, On differential equations of nonlocal elasticity and solutions of screw dislocation and surface waves, *Journal of Applied Physics* **54**: 4703-4710.
- [15] Eringen A.C., 2002, *Nonlocal Continuum Field Theories*, Springer, New York.
- [16] Peddieson J., Buchanan G.R., McNitt R.P., 2003, Application of nonlocal continuum models to nanotechnology, *International Journal of Engineering Science* **41**: 305-312.
- [17] Sudak L.J., 2003, Column buckling of multiwalled carbon nanotubes using nonlocal continuum mechanics, *Journal of Applied Physics* **94**: 7281.
- [18] Ece M.C., Aydogdu M., 2007, Nonlocal elasticity effect on vibration of in-plane loaded double-walled carbon nanotubes, *Acta Mechanica* **190**: 185-195.
- [19] Lu P., Lee H.P., Lu C., Zhang P.Q., 2007, Application of nonlocal beam models for carbon nanotubes, *International Journal Solids and Structures* **44**: 5289-5300.
- [20] Aydogdu M., 2009, Axial vibration of the nanorods with the nonlocal continuum rod model, *Physica E* **41**: 861-864.
- [21] Hu Y., Liew K.M., Wang Q., He X.Q., Yakobson B.I., 2008, Nonlocal shell model for elastic wave propagation in single-and double-walled carbon nanotubes, *Journal of the Mechanics and Physics of Solids* **56**: 3475-3485.
- [22] Sakhae-Pour A., 2009, Elastic buckling of single-layer grapheme sheet, *Computational Materials Science* **45**: 266-270.
- [23] Aydogdu M., 2009, A general nonlocal beam theory: Its application to nanobeam bending, buckling and vibration *Physica E* **41**: 1651-1655.
- [24] Simsek M., Yurtcu H., 2012, Analytical solutions for bending and buckling of functionally graded nanobeams based on the nonlocal Timoshenko beam theory, *Composite Structures* **97**: 378-386.
- [25] Byrd L.W., Birman V., 2007, Modeling and analysis of functionally graded materials and structures, *Applied Mechanics Reviews* **60**: 195-216.
- [26] Rahmani O., Pedram O., 2014, Analysis and modeling the size effect on vibration of functionally graded nanobeams based on nonlocal Timoshenko beam theory, *International Journal of Engineering Science* **77**: 55-70.
- [27] Ebrahimi F., Rastgoo A., Atai A., 2009, A theoretical analysis of smart moderately thick shear deformable annular functionally graded plate, *European Journal of Mechanics-A/Solids* **28**(5): 962-973.
- [28] Ebrahimi F., Naei M.H., Rastgoo A., 2009, Geometrically nonlinear vibration analysis of piezoelectrically actuated FGM plate with an initial large deformation, *Journal of Mechanical Science and Technology* **23**(8): 2107-2124.
- [29] Ghadiri M., 2017, On size-dependent thermal buckling and free vibration of circular FG Microplates in thermal environments, *Microsystem Technologies* **23**: 4989-5001.
- [30] Shafiei N., Ghadiri M., Mahinzare M., 2017, Flapwise bending vibration analysis of rotary tapered functionally graded nanobeam in thermal environment, *Mechanics of Advanced Materials and Structures* **26**: 139-155.
- [31] Reddy J.N., Chin C.D., 1998, Thermomechanical analysis of functionally graded cylinders and plates, *Journal of Thermal Stresses* **21**: 593-626.
- [32] Praveen G.N., Reddy J.N., 1998, Nonlinear transient thermoelastic analysis of functionally graded ceramic-metal plates, *International Journal Solids and Structures* **35**(33): 4457-4476.
- [33] Pisano A.A., Sofi A., Fuschi P., 2009, Nonlocal integral elasticity: 2D finite element based solutions, *International Journal of Solids and Structures* **46**: 3836-3849.
- [34] Pisano A.A., Sofi A., Fuschi P., 2009, Finite element solutions for nonhomogeneous nonlocal elastic problems, *Mechanics Research Communications* **36**: 755-761.
- [35] Eltaher M.A., Samir A.E., Mahmoud F.F., 2013, Static and stability analysis of nonlocal functionally graded nanobeams, *Composite Structures* **96**: 82-88.
- [36] Song M., Yang J., Kitipornchai S., 2018, Bending and buckling analyses of functionally graded polymer composite plates reinforced with graphene nanoplatelets, *Composites Part B: Engineering* **134**: 106-113.

- [37] Wu H., Kitipornchai S., Yang J., 2017, Thermal buckling and postbuckling of functionally graded graphene nanocomposite plates, *Materials& Design* **132**: 430-441.
- [38] Khanchehgardan A., Rezazadeh G., Shabani R., 2013, Effect of mass diffusion on the damping ratio in a functionally graded micro-beam, *Composite Structures* **106**: 15-29.
- [39] Zhen W., Wanji C., 2006, A higher-order theory and refined three-node triangular element for functionally graded plates, *European Journal of Mechanics-A/Solids* **25**(3): 447-463.
- [40] Reddy J., 2000, Analysis of functionally graded plates, *International Journal of Numerical Methods Engineering* **47**(1-3): 663-684.
- [41] Ke L-L., Wang Y-S., Yang J., Kitipornchai S., 2012, Nonlinear free vibration of size-dependent functionally graded microbeams, *International Journal of Engineering Science* **50**(1): 256-267.
- [42] Jia X., Ke L., Feng C., Yang J., Kitipornchai S., 2015, Size effect on the free vibration of geometrically nonlinear functionally graded micro-beams under electrical actuation and temperature change, *Composite Structures* **133**: 1137-1148.
- [43] Li L., Hu Y., 2017, Post-buckling analysis of functionally graded nanobeams incorporating nonlocal stress and microstructure-dependent strain gradient effects, *International Journal of Mechanical Sciences* **120**: 159-170.
- [44] Chen D., Yang J., Kitipornchai S., 2017, Nonlinear vibration and postbuckling of functionally graded graphene reinforced porous nanocomposite beams, *Composites Science and Technology* **142**: 235-245.
- [45] Arbind A., Reddy J., 2013, Nonlinear analysis of functionally graded microstructure-dependent beams, *Composite Structures* **98**: 272-281.
- [46] Reddy J.N., 2011, Microstructure-dependent couple stress theories of functionally graded beams, *Journal of the Mechanics and Physics of Solids* **59**: 2382-2399.
- [47] Yang J., Wu H., Kitipornchai S., 2017, Buckling and postbuckling of functionally graded multilayer graphene platelet-reinforced composite beams, *Composite Structures* **161**: 111-118.
- [48] Wu H., Kitipornchai S., Yang J., 2017, Thermal buckling and postbuckling of functionally graded graphene nanocomposite plates, *Materials& Design* **132**: 430-441.
- [49] Simsek M., 2015, Size dependent nonlinear free vibration of an axially functionally graded (AFG) microbeam using he's variational method., *Composite Structures* **131**: 207-214.
- [50] Ke L-L., Yang J., Kitipornchai S., Wang Y-S., 2014, Axisymmetric postbuckling analysis of size-dependent functionally graded annular microplates using the physical neutral plane, *International Journal of Mechanical Sciences* **81**: 66-81.
- [51] Ke L-L., Yang J., Kitipornchai S., Bradford M.A., 2012, Bending, buckling and vibration of size-dependent functionally graded annular microplates, *Composite Structures* **94**(11): 3250-3257.
- [52] Kitipornchai S., Ke L., Yang J., Xiang Y., 2009, Nonlinear vibration of edge cracked functionally graded timoshenko beams, *Journal of Sound and Vibration* **324**(3): 962-982.
- [53] Farokhi H., Ghayesh M.H., Gholipour A., 2017, Dynamics of functionally graded micro-cantilevers, *International Journal of Mechanical Sciences* **115**: 117-130.
- [54] Shafiei N., Kazemi M., 2017, Nonlinear buckling of functionally graded nano-/micro-scaled porous beams, *Composite Structures* **178**: 483-492.
- [55] Lee J.W., Lee J.Y., 2017, Free vibration analysis of functionally graded bernoulli-euler beams using an exact transfer matrix expression, *International Journal of Mechanical Sciences* **122**: 1-17.
- [56] Tianzhi Y., Ye T., Qian L., Xiao-Dong Y., 2018, Nonlinear bending, buckling and vibration of bi directional functionally graded nanobeams, *Composite Structures* **204**: 313-319.
- [57] Leissa A.W., 1986, Conditions for laminated plates to remain flat under inplane loading, *Composite Structures* **6**(4): 262-270.
- [58] Leissa A.W., 1987, A review of laminated composite plate buckling, *Applied Mechanics Reviews* **40**(5): 575-591.
- [59] Qatu M.S., Leissa A.W., 1993, Buckling or transverse deflections of unsymmetrically laminated plates subjected to in-plane loads, *AIAA Journal* **31**(1): 189-194.
- [60] Shen H.S., 2004, Bending, buckling and vibration of functionally graded plates and shells, *Advances in Mechanics* **34**(1): 53-60.
- [61] Aydogdu M., 2008, Conditions for functionally graded plates to remain flat under inplane loads by classical plate theory, *Composite Structures* **82**: 155-157.
- [62] Shen H.S., 2002, Nonlinear bending response of functionally graded plates subjected to transverse loads and in thermal environments, *International Journal of Mechanical Sciences* **44**: 561-584.
- [63] Ma L.S., Wang T.J., 2003, Axisymmetric post-buckling of a functionally graded circular plate subjected to uniformly distributed radial compression, *Materials Science Forum* **423-424**: 719-724.
- [64] Ma L.S., Wang T.J., 2003, Nonlinear bending and post-buckling of a functionally graded circular plate under mechanical and thermal loadings, *International Journal of Solids and Structures* **40**(13-14): 3311-3330.
- [65] Ma L.S., Lee D.W., 2011, A further discussion of nonlinear mechanical behavior for FGM beams under in-plane thermal loading, *Composite Structures* **93**: 831-842.
- [66] Wang Q., Wang C.M., 2007, The constitutive relation and small scale parameter of nonlocal continuum mechanics for modelling carbon nanotubes, *Nanotechnology* **18**: 075702.